UNDER PEER REVIEW

Porous Ceramics with Directional Pores

ABSTRACT

This chapter describes the results of the authors' previous work on the formation mechanism of porous ceramics using the solidification method. When the coagulation method is adopted as a method for producing porous ceramics, the porous structure can be controlled by the experimental conditions such as solidification rates, atmosphere, total and/or partial pressure of the atmosphere gas, etc. In this chapter, (1) the formation mechanism of porous ceramics with bi-modal pores in shape using unidirectional solidification of water will be described in detail and (2) the formation mechanism of porous alumina by unidirectional solidification in a hydrogen gas atmosphere. In term (1), the following details are provided. Porous ceramics with cylindrical pores were prepared by unidirectional solidification of aqueous slurry containing CO_2 gas, vacuum freeze-drying and sintering. Cylindrical pores were formed during unidirectional solidification under reduced pressure. The solid phase part is a composite of ice and ceramic powder. Porous ceramics with cylindrical pores and fine interconnected pores were obtained by removing only the ice by vacuum freeze-drying and sintering at 1250°C for 5 hours. Porosity and pore size were well controlled by pressure during solidification and firing temperature and time. In term (2), the following details are provided. Porous alumina with a large number of cylindrical pores was prepared by a unidirectional solidification process in a pressurized hydrogen atmosphere. The porous structure is formed at the solid-liquid interface due to the solubility difference of hydrogen between the solid and liquid phases at the melting point. Hydrogen gas dissolves in the molten alumina according to Sievert's law, and insoluble gas corresponding to the solubility gap amount is generated from the solid phase near the solid-liquid interface during unidirectional solidification process, then cylindrical pores are formed. When the ambient gas is pure hydrogen or hydrogen-argon mixture gas, the porosity and pore size of the solidified samples decreased with increasing the total pressure. According to Boyle's law, there is an inverse proportional relationship between the volume of pores and total pressure. In addition, the effects of additives on pore formation are described. The additives are intended to improve the strength of the porous alumina. For the oxides with solubility gap between solid and liquid phase at melting point, cylindrical pores are formed by the solidification process by the same mechanism.

Keywords: Porous ceramics, Solidification process, Micro-structure control, Cylindrical Pores

1. INTRODUCTION

1.1 Background to development of fabrication method of porous ceramics

It is known that bricks have been used since 7000 BC. At that time, bricks were made by drying clay under the sun. Fired bricks, which were heated by fire, are known from the Egyptian civilization 3500 BC. As the product is obtained by firing an oxide, fired bricks fit the definition of ceramics. Presumably, the origin of porous ceramics can be traced to Egypt before 3500 BC. Refractory bricks have undergone significant development since the Industrial Revolution. Refractory bricks have developed because of the need for thermal insulation, heat resistance, refractoriness and corrosion resistance in the inner walls of blast furnaces and industrial furnaces in steel mills. The earliest academic literature is not certain, but the earliest patent is thought to be a patent of US1410729A in 1918 [1]. The first academic literature and patents are not certain, as the fired bricks was so familiar. Subsequently, bricks with superior heat resistance, mechanical properties and durability were developed and many patents were filed. Since the 1960s, many patents have been granted worldwide. Mainly based on the invention of bricks with improved durability and heat resistance [2,3]. The fabrication method of the refractory brick is a type of spacer method, as porous materials are obtained by firing straw and other materials mixed in the clay. The preparation of porous materials using the spacer method allows porosity and pore size to be controlled over a wide range, resulting in porous materials with a relatively homogeneous structure. Therefore, a number of studies have been conducted on improving the spacer method as a method for producing porous materials with the desired mechanical properties and physical performance. For example, Mabuchi et al. devised a heat treatment method based on the spacer method to produce porous copper with excellent compressive properties [4]. In the fabrication of porous ceramics using the spacer method, a sponge or Styrofoam is used as a mold to impregnate the powder slurry, after which the sponge or Styrofoam is removed by sintering [5]. The production of porous materials using the spacer method is still being researched and developed in the field of metals and ceramics, as it is simple and can yield relatively homogeneous and fine porous structures. As the fracture toughness value of ceramics is about 1/10 that of metals, the pores size larger than 50 μm will be an origin of fracture. Therefore, when porous ceramics with relatively large pores are used as an industrial material, the pores must be directional and used to add stress in a direction that does not reduce specific strength. Diesel Particulate Filter (DPFs) and other various filters are in practical use as ceramics with directional pores. In the production of DPFs, clay is extruded to obtain a porous structure. DPFs were put into practical use in 1985 by Mercedes-Benz diesel engine vehicles in US market. The first patent for DPFs was filed by GM in 1981 [6].

1.2 Examples of previous studies on porous ceramics with directional pores

When porous ceramics with macro-pores are used as an industrial material, it is necessary to consider the directionality of the pore shape and the direction of stress loading during use to ensure that the pores do not become an origin of fracture as described above. Prior work on porous ceramics with directional pores includes a freeze-drying method of aqueous slurries and subsequent sintering to produce porous ceramics with directional pores [7,8]. In these methods, the porosity can be controlled by the ratio of oxide powder in the aqueous slurry and/or aqueous gel [7-12]. Since the fusion entropy of H_2O is 2.7R which is almost same to typical oxides such as Al_2O_3, the crystallized ice has facet structure. Hence the porous ceramics prepared by freeze-drying method of aqueous slurries and subsequent sintering shows facet structure. In faceted structures, many areas of stress concentration appear. Therefore, it is necessary to devise ways to prevent the formation of facet structures. Fukushima et al. tried to prepare the porous ceramics without facet structure through the freeze-drying method by adding an antifreeze agent [13]. In general, it is known that the orientation of the ice crystal is suppressed in the solidification of sugar water. This is thought to be due to the large sugar molecules, which inhibit ice facet growth. Fukushima et al. proposed a method to control ice facet growth by controlling the physical properties of water by adding Antifreeze Protein to water [13]. This chapter details the author's previous experiments in which he used the formation of pores during the solidification of carbonated water to suppress ice facet growth. If you look closely at freezer ice, you will see a series of pores. CO_2 is soluble in water, but the solubility of CO_2 in water is higher than the solubility of CO_2 in ice, so when water freezes, excess CO_2 is released. Ice can be described as pseudo-unidirectional solidification, as crystals start to grow from the walls of the ice-maker. In the previous study, the authors proposed a method for producing porous materials with suppressed ice facet growth by utilizing the release of CO_2 gas during solidification. As a result, directional pores are formed. The bimodal porous ceramics can be obtained by freeze-drying method [14,15].

1.3 Other porous materials with directional pores

Other materials or minerals with directional pores exist. Lotus-type porous metals with a large number of aligned cylindrical pores are an example [16,17]. In metal casting technology, the formation of shrinkage cavity is a major problem [18]. The shrinkage cavity is caused by solidification shrinkage and therefore form in the center of the casting. On the other hand, fine porosity may also occur at the boundary between the casting and the mold [19]. Nakajima et al. considered that these pores were formed due to the release of gases dissolved in the molten metal during solidification [17]. As the solubility of hydrogen gas in the liquid metal phase is generally greater than that in the solid phase [20], when a molten metal solidifies under pressurized hydrogen atmosphere, gas corresponding to the gas solubility difference between the solid and liquid phases at the melting point is released from the solid-liquid interface. Solidification in one direction forms cylindrical pores extending in the solidification direction [16,17]. Since the saturation solubility curves of hydrogen gas in the liquid and solid phases of many metals have been established as basic data, it has become possible to predict to some extent whether metals with hydrogen gas solubility differences at the melting point will become porous or not [17]. The formation of Lotus-type porous structures is expected to be possible for non-metals as well, provided that a gas solubility difference exists at the melting point. Non-metallic examples include Lotus-type porous silicon [21], which uses hydrogen gas solubility differences at the melting point, and Lotus-type porous ice [22], which uses carbon dioxide solubility differences at the freezing point. When the same principle is applied to ceramics, non-oxide ceramics such as nitrides or carbides are expected to be difficult to prepare by the solidification method because they decompose or sublimate at high temperatures. However, it is expected that the equivalent principle can be applied to oxides. Although some information is known on the dissolution of water vapor or carbon dioxide gas into magmas [23], there are no reports on gas dissolution into oxide melts in general. The dissolution of water vapor into magmas provides a clue to understanding hydrogen gas dissolution into oxide melts. When water vapor dissolves into magma, water molecules are thought to combine with oxygen ions in the melt to form OH^- ions, as shown in the following equation [23].

$$H_2O + O^{2-} = 2OH^- \qquad (1).$$

The equilibrium constant K can be expressed as $K = \frac{[OH^-]^2}{[H_2O][O^{2-}]}$. If $[O^{2-}]$ is set to 1 because it is an amount that does not change with the concentration of oxygen ions in the melt, the amount of water vapor $[OH^-]$ dissolved into the magma is $[OH^-] = K\sqrt{p_{H_2O}}$, which is known to be proportional to the square root of the water vapor pressure [23]. Although a quasi-binary state diagram for the oxide-hydrogen system has not been established, it is easily inferred from the example of water vapor dissolving into magma that hydrogen combines with oxygen ions in the oxide melt and dissolves into the melt as OH^- ions. Although the existence of solubility differences has not been investigated in detail, it is known that basalt (crystalline due to its high alumina content) becomes porous structure when magma that has flowed to the surface as a lava flow solidifies [24]. This means that gas is released when magma containing volatile components such as water vapor solidifies or solidifies under atmospheric or near-atmospheric pressure and a gas solubility difference is expected to exist between solid and liquid phases at the melting point even for oxides.

With reference to the above previous studies, the authors attempted unidirectional solidification of alumina in high-pressure hydrogen and showed that it is possible to form Lotus-type porous alumina with numerous aligned cylindrical pores, similar to Lotus-type porous metals [25]. This chapter provides details and future suggestions.

2. METHODOLOGY

2.1 Method for preparation of porous ceramics by freeze-drying of aqueous slurry with CO_2 gas

The experimental methodology of this section is detailed in reference [15].

Unidirectional solidification of water containing CO_2 gas forms cylindrical pores [22]. To investigate the pore formation mechanism, unidirectional solidification experiment of water containing CO_2 gas was

carried out. CO_2 gas was poured into distilled water for 30 minutes and the water was poured into a mold. The mold bottom and side walls consisted of copper and transparent acrylic plates, as shown in Figure 1. The copper plate at the bottom of the mold was brought into contact with cooled ethanol. The temperature of the ethanol was kept constant at -50°C. Unidirectional solidification of water starts at the bottom of the mold. The pressure during solidification was controlled by the height of the water, as shown in Figure 1.

In this experiment, Okubo pottery stone powder from Fukushima Prefecture was used. The main component of this mineral is feldspar. The feldspar powder was added to distilled water and CO_2 gas was flowed into the slurry for 30 min while stirring. The slurry was injected into a mold. The bottom and side walls of the mold consisted of copper plates and insulation. The mold was placed statically in a reduced-pressure chamber, as shown in Figure 2, with the bottom of the mold in contact with cooled ethanol. The temperature of the ethanol was kept constant at -50°C. Unidirectional solidification of aqueous slurry occurs from the bottom of the mold. The pressure during solidification was adjusted by an aspirator to achieve a specified reduced pressure. The mixture of solidified ice and oxide powder was freeze-dried for 10 hours to obtain a porous material with a combination of cylindrical pores and connecting pores. Sintering was carried out at 1250 °C for 5 h in air. The porosity of the sintered bulk was measured by the Archimedes method.

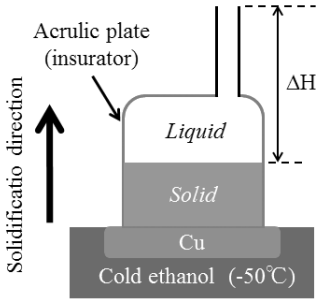

Figure 1 The configuration of the mold using the unidirectional solidification of water [15].

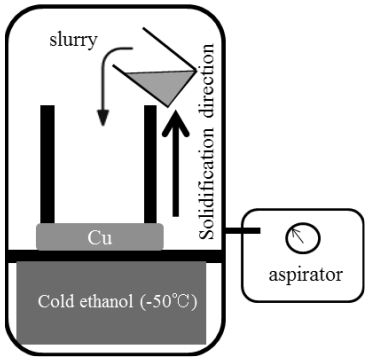

Figure 2 The configuration of the mold using the unidirectional solidification of slurry [15].

2.2 Method for preparation of Lotus-type porous alumina by unidirectional solidification under pressurized hydrogen gas

Details of the experimental methods described in this section are given in detail in reference [25,26]

In general, oxides are reduced at high temperatures. Figure 3 shows the temperature dependence of the free energy change during the reduction reaction for typical oxides [26,27]. The calculation of the free energy change was carried out using the thermodynamic calculation software “FactSage” [28]. For all oxides, the free energy change decreases with increasing temperature. The authors first focused on alumina as an oxide that is not easily reduced at high temperatures and does not absorb atmospheric gases during the cooling process after solidification is complete. Unidirectional solidification was carried out using a floating zone apparatus as shown in Figure 4. The upper and lower shafts were rotated in opposite directions at 20 rpm each. The solidification rate was kept constant at 56 μm/s. A xenon lamp is placed at one of the two foci in the elliptical mirror and the sample is melted at the other focal point.

Hydrogen or a hydrogen-argon mixed gas was used as the atmosphere. However, solidification experiments were carried out in an argon atmosphere when nonporous materials were produced. Sintered alumina of 4N purity were used as feed rod. The effect of adding silica (SiO_2) and calcia (CaO) on the solidification and formation of pores was investigated.

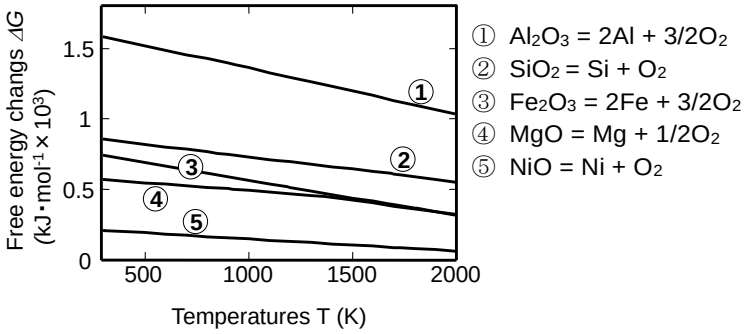

Figure 3 Free energy changes with reduction reactions for some typical oxides [26].

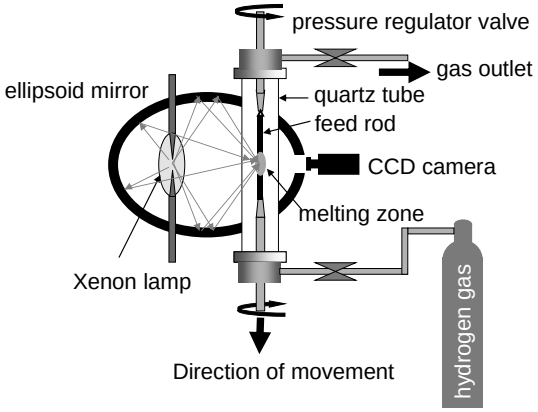

Figure 4 Schematic diagram of the floating zone apparatus.

3. RESULTS AND DISCUSSION

3.1 Formation of cylindrical pores by unidirectional solidification of carbonated water

Murakami et al. reported the formation of cylindrical pores by unidirectional solidification of carbonated water [22]. Figures 5(a) and (b) show ice obtained by solidification of carbonated water in one direction under pressures of 0.10 MPa and 0.11 MPa [14,15]. The pore diameters of these samples were 70.97 and 37.10 μm, respectively. Pore diameter was measured at 4.4 mm above the bottom of the mold, as pores are not formed near the bottom of the mold. A similar trend has been observed during the fabrication of Lotus-type porous metals by the mold casting method [17,29]. Pore diameter decreases rapidly with slight increases in pressure. Figure 6 shows the diameter of cylindrical pores. Here, the d^3 dimension, i.e. the volume dimension, is shown in relation to pressure. The pore volume decreases with increasing pressure. A similar trend is observed in Lotus-type porous metals prepared by unidirectional solidification under pressurized hydrogen gas [17,29]. The formation mechanism of the directional pores for Lotus-type porous metals is considered to be based on a model in which, during unidirectional solidification, excess hydrogen atoms diffuse and flow into the pores in the solid phase near the solid-liquid interface and pores grow, as shown in Figure 7. In this Figure, the upper end of the pore is in contact with the liquid phase, which in turn is in contact with the ambient gas. The pressure inside the pores increases with increasing total pressure according to equation (2). Therefore, the volume of the pore decreases with increasing total pressure according to Boyle's law.

$$P = \frac{2\gamma}{R} + P_0 \qquad (2)$$

Where P, γ, R and P_O are the pressure inside the pore, the surface tension of the liquid phase, the radius of curvature of the pore and the total pressure, respectively.

Figure 8 shows the solid-liquid interface morphology of pores obtained by unidirectional solidification of carbonated water. The morphology of the solid phase, liquid phase and pores is the same as that in Figure. 7, which suggests that the formation mechanism of the cylindrical pores shown in Figure. 5(a) and (b) is the same as that of the Lotus-type porous metals. The diameter of the cylindrical pores in Lotus-type porous metals can be controlled in the pressure range from 0.1 to 1.0 MPa [15]. In contrast, in the present study, the pore dimensions are significantly reduced in a very narrow pressure range of 0.10 to 0.11 MPa. The surface tension of the liquid phase is closely related to the formation of pores, since the pressure inside the pores can be expressed by equation (2). For example, the surface tension of copper at its melting point is 1306 dyne/cm [30]. On the other hand, the surface tension of water at 20 °C is 72 dyne/cm. According to equation (2), the effect of the total pressure on the pressure inside the pores in the case of molten metal is much smaller than in the case of water. Therefore, when pores are formed by the solidification of carbonate water, a very narrow pressure range is required to control the pore size. These results suggest that precise control of the total pressure during the solidification process is necessary for the preparation of porous ceramics with cylindrical pores by unidirectional solidification using carbonate water.

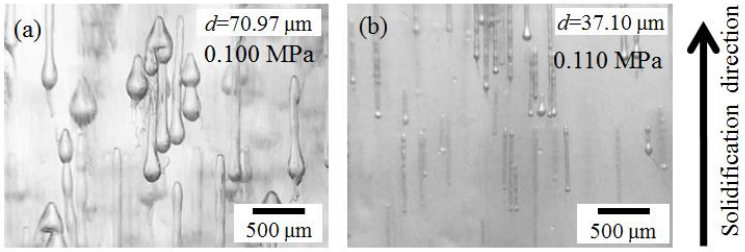

Figures 5 The ice with cylindrical pores solidified under (a) 0.10 and (b) 0.11 MPa [15].

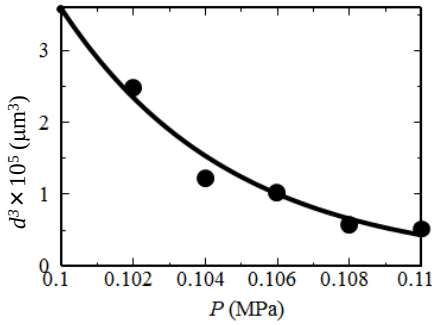

Figure 6 Pressure dependence of pore size [15].

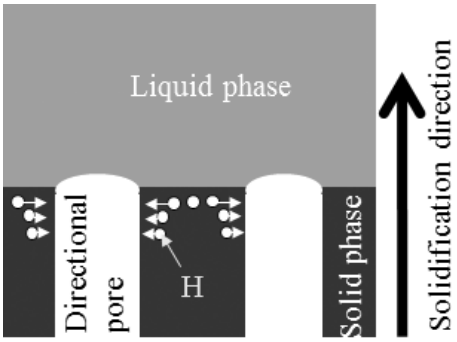

Figures 7 The formation mechanism of directional pores for Lotus-type porous metals in pressurized hydrogen atmosphere [15].

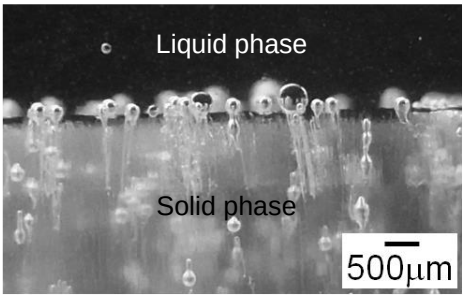

Figure 8 The conFigureuration of solid-liquid interface during the unidirectional solidification of water [15].

3.2 Formation of porous ceramics using the process of unidirectional solidification of carbonated aqueous slurry, freeze-drying and sintering

The porous ceramics were prepared by a process of unidirectional solidification under reduced pressure, freeze-drying and sintering processes. The sintering temperature and time were fixed at 1250°C and 5 hours. Pressures during the solidification were controlled at 0.10, 0.07, 0.05 and 0.03 MPa. Experimental conditions and the porosity of each sample are summarized in Table 1. Cross section views of the sintered samples perpendicular to the solidification direction is shown in Figures 9. In samples C and D, a large number of fine circular pores are observed. Longitudinal views of the sintered samples are shown in Figures 10. In samples C and D, directional pores are observed. Thus, it can be seen that these directional pores have cylindrical shape. For all samples, the shrinkage due to sintering was around 40%. In the case of the samples A and B, no cylindrical pores were formed. As the density of slurry is larger than that of water, the pressure at the interface between the liquid phase and the pores is greater than 0.1 MPa. It is considered that cylindrical pores do not form under a pressure of 0.1 MPa. Figures 11 (a) and (b) show SEM images of cross sections of sample A perpendicular and parallel to the solidification direction. Fine directional pores are formed. These pores are thought to have formed during the removal of ice by freeze-drying process. The porosity of this sample was 60.8%. The porosity of each sample is shown in Figure 12. Fine pores are present in all samples; at pressures lower than 0.07 MPa, porosity increases with decreasing pressure. All samples have a porosity of 60%, as all samples have connecting pores formed by the vaporization of ice from the ice/powder complex during the freeze-drying process. On the other hand, the porosity of samples prepared at pressures below 0.07 MPa increases with the formation of cylindrical pores. The formation of cylindrical pores contributes to increasing the porosity of the sample.

In the present study, the slurry concentration and sintering conditions were fixed. The porosity and pore size of the samples can be controlled by the slurry concentration, pressure during solidification, sintering temperature and sintering time. The porosity of the interconnecting pores should be controlled by the volume fraction of water and powder in the slurry. The pore size of the connecting pores and cylindrical pores can also be controlled by the sintering conditions. Furthermore, the fraction of the cylindrical pores can be controlled by the pressure during solidification of the slurry. As regards the pore size, it can be controlled by pressure and sintering conditions. The pore size of the connecting holes can also be controlled by the sintering conditions.

Table 1 The experimental condition for each sample.

Sample	Pressure during the solidification	Sintering temperature (°C) and time (hours)	Porosity
A	0.10 MPa	1250°C× 5 hours	60.8%
B	0.07 MPa		60.9%
C	0.05 MPa		70.6%
D	0.03 MPa		77.8%

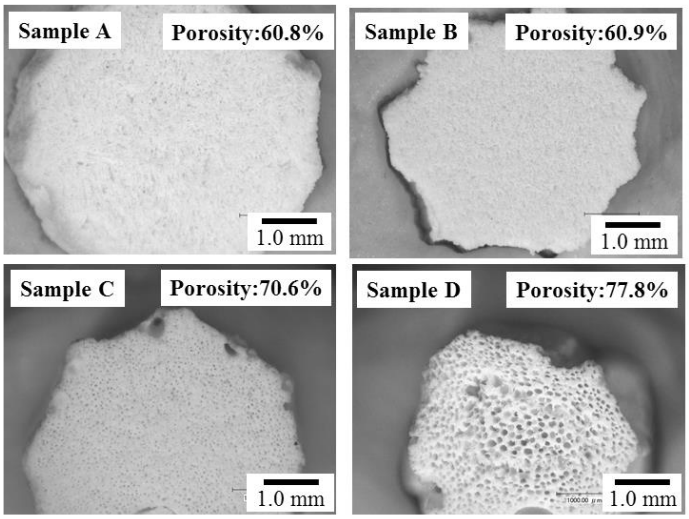

Figures 9 The cross section view of the samples perpendicular to solidification direction [15].

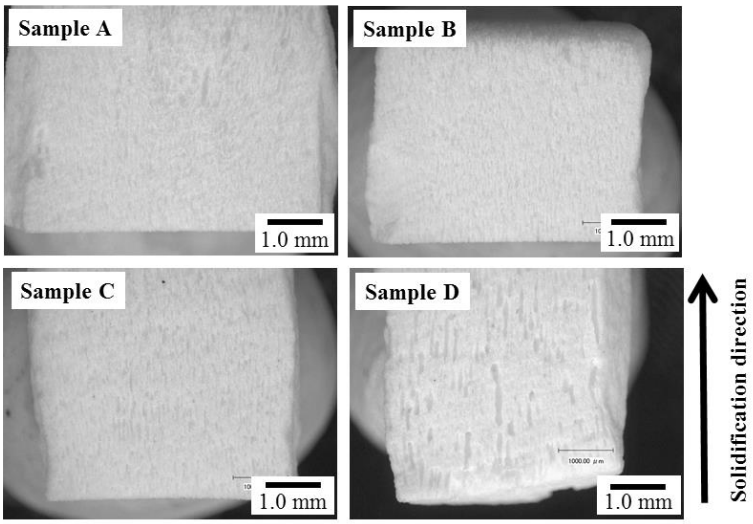

Figures 10 The cross section view of the sintered samples parallel to solidification direction [15].

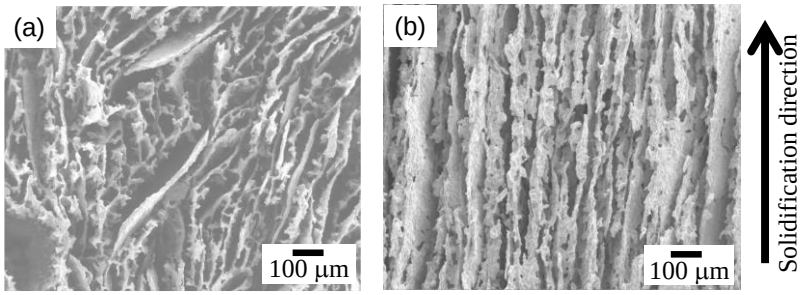

Figures 11 Cross sections of sample A perpendicular and parallel to the solidification direction [15].

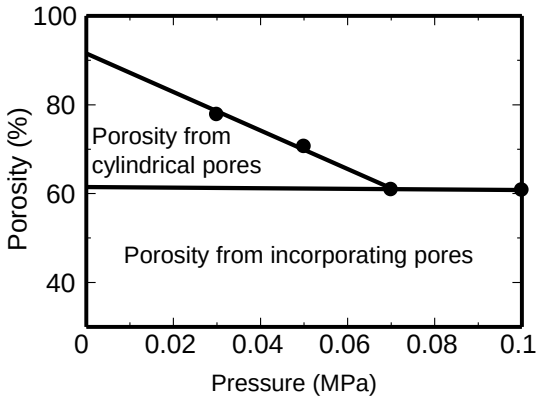

Figure 12 The porosity of each sample [15].

3.3 Formation of Lotus-type porous alumina prepared by unidirectional solidification under pressurized hydrogen gas atmosphere

As an example, the cross sections of the fabricated Lotus-type porous alumina perpendicular and parallel to the solidification direction are shown in Figures 13(a) and 3(b) [25]. The samples were prepared in a mixed gas atmosphere of 50% H_2-50% Ar at 0.8 MPa using alumina feed rods of 4N purity. Lotus-type porous alumina was obtained, which has the same structure as Lotus-type porous metals with numerous cylindrical pores arranged in the solidification direction. The solid-liquid interface at the start of solidification is shown as a dashed line. Due to the convex shape of the solidification interface, pores formed off-center of the sample grow obliquely towards the outside of the sample along the temperature gradient. In the case of Lotus-type porous stainless steels [31] and intermetallic compounds [32] produced by the unidirectional solidification method, the solid-liquid interface geometry is concave, so that pores formed at points away from the center of the sample grow at an angle towards the center of the rod. This structural difference is due to the shape of the solid-liquid interface. In both cases, the pores grow along the temperature gradient. The difference in the shape of the solid-liquid interface between metals and ceramics is considered to be related to the thermal conductivity of the material. Figure 14 shows cross-sections perpendicular to the solidification direction of Lotus-type porous alumina prepared by varying the hydrogen partial pressure and total pressure [25]. Pore diameter and porosity decrease with increasing total pressure. Pore diameter and porosity decrease with decreasing hydrogen partial pressure. The porosity calculated from Figure 14 is shown in Figure 15 [25]. With the exception of the sample prepared at 0.2 MPa using 100% H_2 gas, the porosity decreases with increasing total pressure. Assuming that pores grow at the solid-liquid interface during unidirectional solidification, the pressure P inside the pores depends on the total pressure P_0 according to equation (2) through the liquid phase. Strictly speaking, the first term in equation (2) also increases with the total pressure, since the pore size decreases as the total pressure increases. However, the surface tension of the alumina melt is approximately 0.6 N/m [33] and the change in average pore diameter is about 250 μm when the total pressure changes from 0.2 to 0.8 MPa, so the change in the first term relative to the change in total pressure is about 1/1000 and can be ignored. The pressure in the pore is therefore proportional to the total pressure. The volume of the pores is inversely proportional to the total pressure according to Boyle's law. The solid line in Figure 15 shows the curve obtained by fitting the porosity with the inverse of the total pressure. It can be seen that porosity is inversely proportional to total pressure. These results indicate that the pores of Lotus-type porous alumina are formed at the solid-liquid interface through the liquid phase.

On the other hand, the relationship between porosity and hydrogen partial pressure is shown in Figure 16 [25]. Hydrogen solubility in the alumina solid phase was investigated in detail by Serra et al [34]. The solubility C_s has been reported to be proportional to the hydrogen partial pressure to the power of one-half according to the Sieverts' law. On the other hand, the hydrogen solubility C_m in the alumina liquid phase has not been reported yet. Assuming that C_m follows the Sieverts' law and that a hydrogen gas solubility difference $\Delta C_{m\text{-}s}$ exists at the melting point, $\Delta C_{m\text{-}s}$ is a quantity proportional to the hydrogen partial pressure to the power of one-half. The amount of $C_{m\text{-}s}$ is proportional to the hydrogen partial pressure to the power of one half. In the pore formation mechanism of Lotus-type porous metals, it has

also been reported that not all gases corresponding to hydrogen gas solubility differences contribute to pore formation [35]. About half of the solubility difference gas dissipates into the atmosphere. However, in a steady state of unidirectional solidification, the amount of gas dissipated per unit time is considered to be constant, so the volume of pores formed is proportional to the hydrogen partial pressure to the power of one-half. The solid line in Figure 16 is the result of fitting the porosity with a function proportional to the hydrogen partial pressure to the power of one-half. In all cases, it can be seen that porosity is proportional to the hydrogen partial pressure to the power of one-half. These results suggest that hydrogen solubility in alumina melts follows the Sieverts' law and that hydrogen gas solubility differences exist at the melting point. The pore formation mechanism of Lotus-type porous alumina is similar to that of Lotus-type porous metals, in that gas corresponding to the hydrogen gas solubility difference at the melting point is released from the solid phase during solidification.

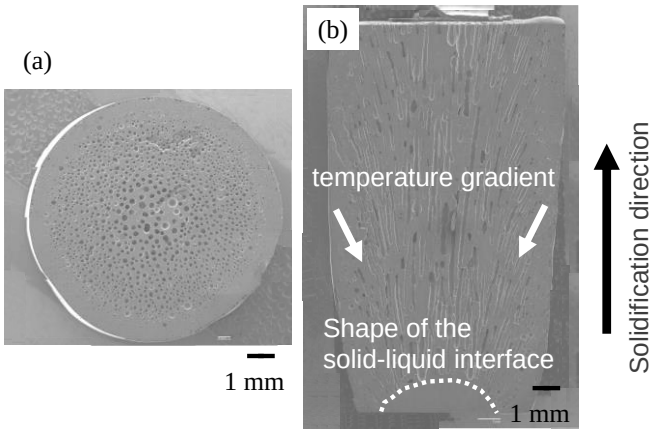

Figures 13 Cross sections views of Lotus-type porous alumina (a) perpendicular and (b) parallel to the solidification direction [25].

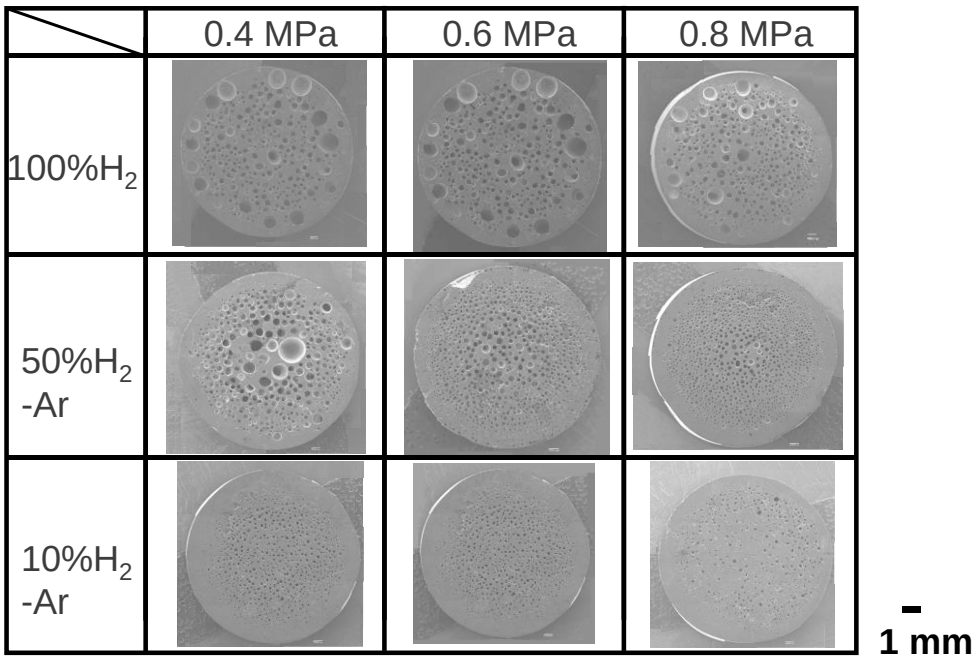

Figures 14 Cross-sections perpendicular to the solidification direction of Lotus-type porous alumina prepared by varying the hydrogen partial pressure and total pressure [25].

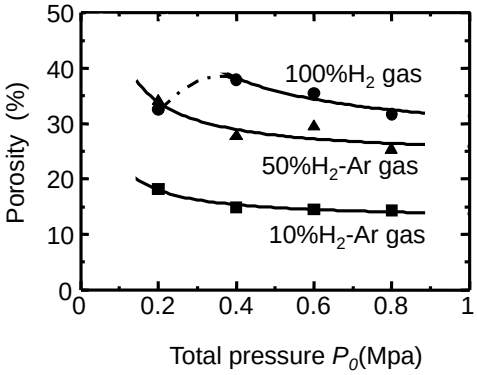

Figure 15 The porosity of each sample calculated using images of Fig.14 [25].

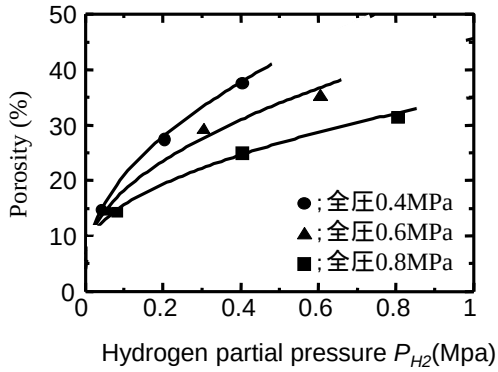

Figure 16 The relationship between porosity and hydrogen partial pressure [25].

3.4 Effect of adding calcia and silica

The formation mechanism for cylindrical pores is described above, and only a portion of the amount of gas corresponding to the solubility difference at the melting point contributes to pore formation. For this reason, a solidification velocity of 56 μm/s was used in the present experiments. This solidification rate is several tens of times faster than the conditions for preparing single oxide crystal. Therefore, grain boundaries are formed in the solidified ceramics. As the raw material is of high purity, there is no glass phase at the grain boundaries and grain boundaries equal to cracks are formed. Therefore, the compressive strength of the non-porous alumina prepared in argon at a solidification rate of 56 μm/s is only 267 MPa, which is about 1/10 of that of commercially available high-strength alumina bulk [36]. In general, the improvement of the properties of ceramics is achieved by controlling the composition, quantity and structure of the boundary phase. To improve the mechanical properties of Lotus-type porous alumina, it is necessary to form boundary glassy phase during the unidirectional solidification process. The authors focused on the composition of sintering aids commonly used in the fabrication of structural ceramics, and attempted to fabricate Lotus-type porous alumina using alumina rods to which silica, calcia and other additives were added, and investigated the effect of the added components on the pore formation. Figure 17 shows the change in porosity of samples prepared in a hydrogen atmosphere at 0.1 MPa with the addition of silica [37]. Porosity increases with silica addition, although the variation in pore size increases. Feed rods with silica additions fixed to a composition of $85Al_2O_3$-$15SiO_2$ were used to prepare solidified samples in a high-pressure hydrogen atmosphere. The cross section perpendicular to the solidification direction is shown in Figure 18 [26, 37]. When the solidification was performed under pressurized hydrogen atmosphere, the pore size heterogeneity disappeared and solidified porous ceramics with an almost uniform pore distribution was obtained. It can be seen that the pore size decreases as the total pressure increases and the pore size and porosity decrease as the hydrogen partial pressure decreases. This trend is the same as when alumina of purity 4N is used as raw material.

No circular pores were formed when solidification is carried out in a low hydrogen partial pressure of 10% H_2-90% Ar atmosphere. When solidified in 50H_2-Ar atmosphere, fine pores are formed. Mullite ($3Al_2O_3$-$2SiO_2$), a complex oxide of alumina and silica, has been reported to produce bubbles due to gasification of the silica component when melted in a reducing atmosphere [38,39]. The fine independent pores seen in Fig. 18 are thought to be formed by the gasification of the silica component, with the fine bubbles generated in front of the solid/liquid interface being incorporated into the solid phase during the unidirectional solidification process. On the other hand, when alumina with calcia additive was solidified in a 0.1 MPa hydrogen atmosphere, the increase in porosity was within 10%. For more information, see reference [26]. Figures 19 show cross-sections perpendicular to the solidification direction of samples prepared using alumina rod with 1%CaO-10%SiO_2 and 1%CaO-20%SiO_2 added [37]. Solidification was carried out at 0.1 MPa hydrogen atmosphere. When silica and calcia are added simultaneously, the porosity increases with the amount of silica added, indicating that a homogenized pore positional distribution is obtained [40]. Elemental analysis of a cross-section perpendicular to the solidification direction of a nonporous solidified alumina prepared from alumina rod with 1%CaO-20%SiO_2 additive under 0.1 MPa Ar atmosphere shows that silica and calcia segregate at the grain boundaries, as shown in Figure 20 [36]. In the powder X-ray diffraction diagram of this sample, only alumina phase was identified as crystalline and a halo pattern characteristic of the silica-based glass phase was observed in the range of 2θ from 15 to 30 degrees. Therefore, the grain boundary phase in Figure 20 is found to be a glass phase composed of silica and calcia. The compressive strength of this sample was 1679 MPa, which was six times higher than that of solidified alumina using 4N purity alumina as a feed rod [36].

It was found that even with the unidirectional solidification process, it is possible to improve the strength of the solidified oxide ceramics by forming a glassy boundary phase at the grain boundaries. This could be a technology for controlling mechanical properties when ceramic materials are prepared by the solidification process in the future.

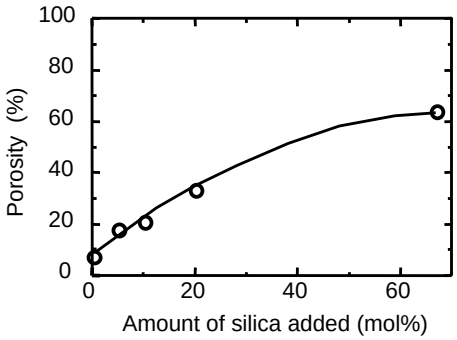

Figure 17 Porosity of samples prepared in a hydrogen atmosphere at 0.1 MPa with the addition of silica [37].

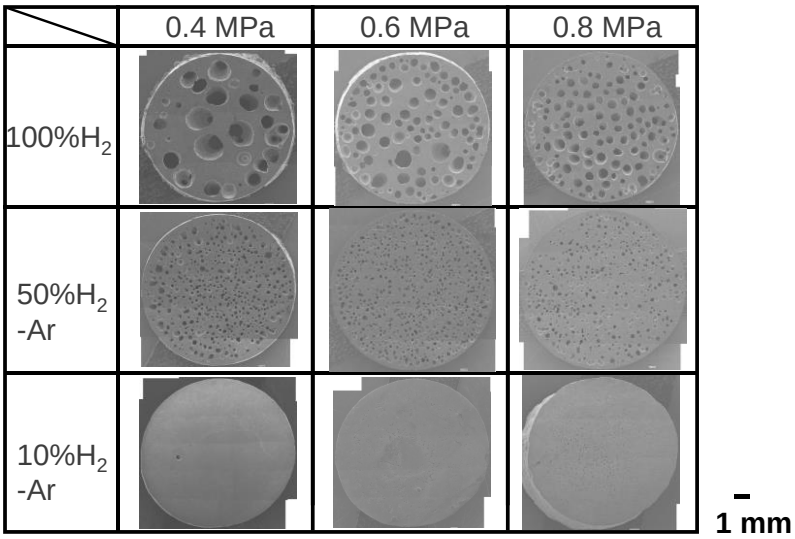

Figures 18 Cross section view of the solidified sample prepared using $85Al_2O_3$-$15SiO_2$ feed rod [37].

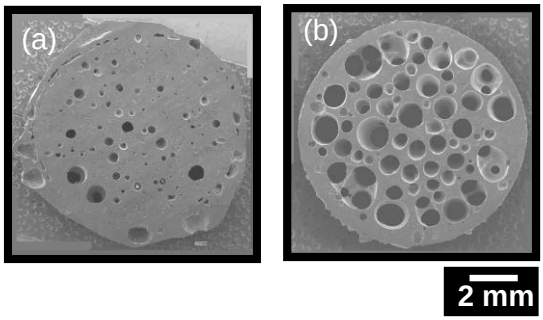

Figures 19 Cross-sections perpendicular to the solidification direction of samples prepared using alumina rod with (a) 1%CaO-10%SiO_2 and (b) 1%CaO-20%SiO_2 added [37].

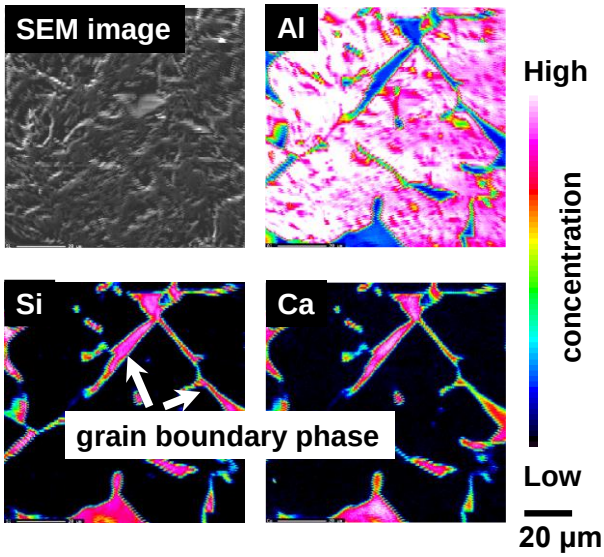

Figure 20 Elemental analysis of nonporous solidified alumina with 1%CaO-20%SiO_2 additive [37].

3.5 Some future suggestions for porous ceramics with directional pores

In this chapter, a method for fabrication of porous ceramics using the release of gases by solidification process was introduced. As shown in equation (1), in oxides, hydrogen is present in the melt as OH^- ions, both when hydrogen is dissolved in the melt and when water vapor is dissolved in the melt. Therefore, it should be possible to prepare Lotus-type porous alumina in a water vapor atmosphere without the use of hydrogen gas. Indeed, the authors have obtained experimental data on the formation of Lotus-type porous alumina by unidirectional solidification in water vapor environment. This will be published as a paper in the near future. Furthermore, carbonising wood yields porous carbon with directional pores. It is reported that when silica is applied to the pore walls the porous carbon and heat treated, silicon carbide ceramics with directional pores can be obtained. The authors have further developed their research methods and set out to develop a technique for the preparation of oxide ceramics with directional pores as like wood. These results will also be published in a paper in near future.

4. CONCLUSION

In this chapter, a new fabrication method for porous alumina with cylindrical pores using unidirectional solidification process. A fabrication process for the porous ceramics with cylindrical pores and incorporating pores was introduced in this chapter. To control the porous structure and porosity, the formation mechanism of cylindrical pores in ice was examined. It can be concluded as follows; (1) The formation of cylindrical pores in ice by unidirectional solidification of water containing CO_2 gas can be controlled by a small pressure range from 0.10 to 0.11 MPa. (2) The formation of cylindrical pores by

unidirectional solidification of slurry containing CO_2 gas can be recognized under reduced pressure.

On the other hand, Lotus-type porous alumina that has number of cylindrical pores can be prepared by unidirectional solidification of alumina feed rod under pressurized hydrogen gas atmosphere. In this method, the porosity and the pore size can be controlled by total pressure and partial pressure of hydrogen gas. The porosity of the solidified samples follows Boyle's law and Sieverts' law. The pore size follows Boyle's law. Furthermore, the pore size distribution homogeneity controlled by the environmental pressure. It is difficult to form boundary glassy phase at grain boundaries during the solidification process because of segregation reactions occurs. However, if the solidification rate is fast, it is possible to form boundary glassy phase in the solidification process by controlling the composition of the additives.

REFERENCES

1. G.A. Balz, “REFRACTORY BRCK”, US Patent, 1410729A (1918).
2. T. Ebina, “BRCK”, Japan Patent, 2339 (1894).
3. O.P. Chawala, “Determination of Thermal-Conductivity of Refractory Bricks by Transient Line Source Method and Its Relationship with Temperature and Porosity”, Indian Journal of Technology, **13**, 2, 80-84 (1975).
4. M. Hakamada,Y. Asao, T. Kuromura, Y. Chen, H. Kusuda, M. Mabuchi, “Density Dependence of the Compressive Properties of Porous Copper over a Wide Density Range”, Acta Materialia, **55**, 7, 2291-2299 (2007).
5. M.A.A.M. Nor, H.M. Akil, Z.A. Ahmad, “The Effect of Polymeric Template Density and Solid Loading on the Properties of Ceramic Foam”, Science of Sintering, **41**, 319-327 (2009).
6. M. Berg and G. Blanc, “Ceramicfilters for Deselexhaust Particulates and Methods for Making”, US Patent, 4,364,761 (1982).
7. S. Deville, “Freeze-casting of Porous Ceramics: A Review of Current Achievements and Issues”, Advanced Engineering Materials, **10**, 3, 155-169 (2008).
8. T. Fukasawa, M. Ando, T. Ohji, S. Kanzaki, “Synthesis of Porous Ceramics with Complex Pore Structure by Freeze-dry Processing”, Journal of the American Ceramic Society, **84**, 1, 230-232 (2001).
9. M.T. Buscaglia, M. Viviani, V. Buscaglia, L. Mitoseriu, A. Testino, P. Nanni, Z. Zhao, M. Nygren, C. Harnagea, D. Piazza, C. Galassi, “High Dielectric Constant and Frozen Macroscopic Polarization in Dense Nanocrystalline $BaTiO_3$ Ceramics”, Physical Review B, **73**, 6, 064114 (2006).
10. M. Fukushima, H. Hyuga, M.C. Matsunaga, Y. Yoshizawa, “Thermal Conductivity Analysis using Three-dimensional Microstructures of Gelation Freezing Derived Cellular Mullite”, Journal of the American Ceramic Society, **101**, 8, 3266-3270 (2018).
11. T. Ohji and M.Fukushima, “Macro-porous Ceramics: Processing and Properties”, International Materials Reviews, **57**, 2, 115-131 (2012).
12. M. Fukushima and Y. Yoshizawa, “Fabrication and Morphology Control of Highly Porous Mullite Thermal Insulators Prepared by Gelation Freezing Route”, Journal of the European Ceramic Society, **36**, 12, 2947-2953 (2016).
13. M. Fukushima, S. Tsuda and Y. Yoshizawa, “Fabrication of Highly Porous Alumina Prepared by Gelation Freezing Route with Antifreeze Protein”, Journal of the American Ceramic Society, **96**, 4, 1029–1031 (2013).
14. J-W Lee, T. Akatsu and S. Ueno, “Fabrication of Porous Ceramics with Bi-modal Pores in Shape by Unidirectional Solidification of Aqueous Slurry Containing CO_2 Gas”, Journal of the Technical Associations of Refractories, Japan, **34**, 4, 226-230 (2014).
15. S. Ueno and J-W Lee, “Bimodal Porous Ceramics Based on the Segregation and Gas-Crystal Reactions Associated with the Solidification of Water”, 26th Annual Scientific Conference of The Technical Association of Refractories Japan, Compendium of Abstracts (2013).
16. H. Nakajima, “Fabrication, Mechanical and Physical Properties, and Its Application of Lotus-Type Porous Metals”, Materials Transactions, **60**, 12, 2481-2489 (2019).
17. H. Nakajima, “Fabrication, Properties and Application of Porous Metals with Directional Pores”,

Progress in Materials Science, **52**, 7, 1091-1173 (2007).
18. M. Hecht, P. Cloarec, “Inoculation of Flake Graphite Cast-Iron and Tendency to Form Shrinkage Cavities-Case of Phosphor Cast-Iron for Thin Casting”, Fonderie, **31**, 352, 3-19 (1976).
19. S.F. Fischer, P.Schueler, C.Fleck, A.B. Polaczek, “Influence of the Casting and Mould Temperatures on the Microstructure and Compression Behaviour of Investment-Cast Ppen-Pore Aluminium Foams”, Acta Materialia, **61**, 14, 5152-5161 (2013).
20. D.P. Smith, “Hydrogen in metals”, The University of Chicago Press, Chicago, p34 (1947).
21. T. Nakahata and H. Nakajima, “Fabrication of Lotus-type Porous Silicon by Unidirectional Solidification in Hydrogen”, Materials Science and Engineering: A, **384**, 1-2, 373-376 (2004).
22. K. Murakami and H. Nakajima, “Formation of Pores during Unidirectional Solidification of Water Containing Carbon Dioxide”, Materials Transactions, **43**, 10, 2582-2588 (2002).
23. Y. Liu, Y. Zhang and H. Behrens, “Solubility of H_2O in Rhyolitic Melts at Low Pressures and a New Empirical Model for Mixed H_2O–CO_2 Solubility in Rhyolitic Melts”, Journal of Volcanology and Geothermal Research, **143**, 1-3, 219-235 (2005).
24. X. Xie, S.L. Fox and G.A. Bala, “Spontaneous Imbibition in Porous Basalt Mediated by Microbial Perturbations”, Journal of Petroleum Science and Engineering, **52**, 1-4, 287-296 (2006).
25. S. Ueno, L.M. Lin and H. Nakajima, “Formation Mechanism of Porous Alumina with Oriented Cylindrical Pores Fabricated by Unidirectional Solidification”, Journal of the American Ceramic Society, **91**, 1, 223-226 (2008).
26. S. Ueno, L.M. Lin and H. Nakajima, “Lotus-type Porous Ceramics Produced by the Unidirectional Solidification Process”, Materia Japan, **47**, 8, 399-405 (2008). (in Japanese)
27. S. Ueno, L.M. Lin and H. Nakajima, “Role of Impurity Additives on Pore Formation of Lotus-type Porous Alumina”, Journal of High Temperature Society, **34**, 2, 51-55 (2008).
28. C.W. Bale, P. Chartrand, S.A. Degtrev, G. Eriksson, K. Hack, R.B. Mahfoud, J. Melancon, A.D. Pelton and S. Petersen, “FactSage thermochemical software and databases”, Calphad, **26**, 2, 189-228 (2002).
29. S.K. Hyun, K. Murakami and H. Nakajima, “Anisotropic Mechanical Properties of Porous Copper Fabricated by Unidirectional Solidification”, Materials Science and Engineering: A, **299**, 1-2, 241-248 (2001).
30. A. Kasama, T. Iida and Z. Morita, “Temperature Dependence of Surface Tension of Liquid ure Metals”, Journal of the Japan Institute of Metals and Materials, **40**, 1030-1038 (1976).
31. T. Ikeda, T. Aoki and H. Nakajima, “Fabrication of Lotus-type Porous Stainless Steel by Continuous Zone Melting Technique and Mechanical Property”, Metallurgical and Materials Transaction A, **36**, 77-86 (2005).
32. S.K. Hyun, T. Ikeda and H. Nakajima, “Fabrication of Lotus-type Porous Ni_3Al Intermetallics”, Journal of the Japan Institute of Metals, **68**, 2, 39-42 (2004).
33. P.F. Paradis and T. Ishikawa, “Surface Tension and Viscosity Measurements of Liquid and Undercooled Alumina by Containerless Techniques”, Japanese Journal of Applied Physics, **44**, 5082-5085 (2005).
34. E. Serra, A.C. Bini, G. Cosoli and L. Pillioni, “Hydrogen Permeation Measurements on Alumina”, Journal of the American Ceramic Society, **88**, 1, 15-18 (2005).
35. S. Yamamura, H. Shiota, K. Murakami and H. Nakajima, “Evaluation of Porosity in Porous Copper Fabricated by Unidirectional Solidification under Pressurized Hydrogen”, Materials Science and Engineering: A, **318**, 1-2, 137-143 (2001).
36. S. Ueno, L.M. Lin, H. Nakajima, E. Yasuda, “Effects of Impurities on Formation Pores during Solidification for Porous Alumina and Its Compressive Strength”, Journal of the Ceramic Society of Japan, **116**, 1, 137-140 (2008).
37. S. Ueno, L.M. Lin and H. Nakajima, “A New Fabrication Method of Porous Ceramics using Unidirectional Solidification”, Advanced in Science and Technology, **45-53**, 799-802 (2006).
38. R.F. Davis, I.A. Aksay and J.A.Pask, “Diffusion and Reaction Studies in the System Al_2O_3-SiO_2”, Journal of the American Ceramic Society, **55**, 10, 98-101 (1972).
39. Z. Xiao and B.S. Mitchell, “Mullite Decomposition Kinetics and Melt Stabilization in the Temperature Range 1900 – 2000 °C”, Journal of the American Ceramic Society, **83**, 4, 761-767 (2000).
40. S. Ueno, L.M. Lin and H. Nakajima, “Effect of Impurities on Formation of Pores in Porous Alumina during Unidirectional Solidification”, Materials Science Forum, **569**, 313-316, (2008).